JOURNAL OF TISSUE ENGINEERING AND REGENERATIVE MEDICINE
J Tissue Eng Regen Med 2016; **10**: 669–678.
Published online 29 October 2013 in Wiley Online Library (wileyonlinelibrary.com) **DOI:** 10.1002/term.1840

RESEARCH ARTICLE

Size matters: effects of PLGA-microsphere size in injectable CPC/PLGA on bone formation

Hongbing Liao[1,2†], Rosa P. Félix Lanao[1†], Jeroen J. J. P. van den Beucken[1], Nuo Zhou[2], Sanne K. Both[1], Joop G. C. Wolke[1] and John A. Jansen[1*]

[1]*Department of Biomaterials, Radboud University Nijmegen Medical Centre, Nijmegen, The Netherlands*
[2]*College of Stomatology, Guangxi Medical University, Nanning, People's Republic of China*

Abstract

The aim of this study was to evaluate the effect of PLGA microsphere dimensions on bone formation after injection of calcium phosphate cement (CPC)/PLGA in a guinea pig tibial intramedullarly model. To this end, injectable CPC/PLGA formulations were prepared using PLGA microspheres with either a small (~25 μm) or large (~100 μm) diameter, which were incorporated at a 20:80 ratio (wt%) within apatite CPC. Both CPC/PLGA formulations were injected into a marrow-ablated tibial intramedullary cavity and, after an implantation period of 12 weeks, histology and histomorphometry were used to address bone formation. The results demonstrated bone ingrowth throughout the entire scaffold material for both CPC/PLGA formulations upon PLGA microsphere degradation. More importantly, bone formation within the CPC matrix was > two-fold higher for CPC-PLGA with 25 μm PLGA microspheres. Additionally, the pattern of bone and marrow formation showed distinct differences related to PLGA microsphere dimension. In general, this study demonstrates that PLGA microsphere dimensions of ~25 μm, leading to pores of ~25 μm within CPC, are sufficient for bone ingrowth and allow substantial bone formation. Further, the results demonstrate that PLGA microsphere dimensions provide a tool to control bone formation for injectable CPC/PLGA bone substitutes.

Received 9 October 2012; Revised 13 February 2013; Accepted 13 September 2013

Keywords **calcium phosphate cement; microspheres; size; PLGA; biodegradation; animal model**

1. Introduction

With an estimated annual number of ~2.5 million procedures, bone grafting has become a substantial surgical intervention in medical and dental healthcare (Kolk *et al*., 2012). Although autografts represent the primary choice for a grafting material, issues related to autograft availability and quality urge for alternatives.

From a practical point of view, the use of synthetic bone substitutes for bone-regenerative treatments has several advantages over autografts, including off-the-shelf availability and minimal patient discomfort, as no additional surgery is necessary to harvest autologous bone. Additionally, the application of the bone substitute material should be simple and effective, meaning that material preparations within the operating theatre do not involve cumbersome steps and that the handling properties of the bone substitute material allow the bone defect to be perfectly filled. In this respect, injectable bone substitute materials are appealing for reasons of their syringe-based application via minimally invasive surgery and their capacity to optimally fill irregularly-shaped defects (Kretlow *et al*., 2009; Bongio *et al*., 2010).

In view of the composition of such synthetic bone substitutes, calcium phosphate (CaP)-based ceramics are well known for their superior biological performance in bone-regenerative approaches (Dorozhkin 2010). In an injectable form, CaP cements (CPCs) were introduced by Brown and Chow (1986). Such CPCs are currently available with either brushite (Tamimi *et al*., 2012) or apatite (Bohner, 2010) as the main end-product. Although brushite CPCs are readily degradable, their low mechanical properties limit their wide application. On the other hand, apatite CPCs have higher mechanical properties, but their slow degradation limits timely full replacement by newly formed bone tissue.

**Correspondence to: John A. Jansen, Department of Biomaterials, 309 Radboud University Nijmegen Medical Centre, PO Box 9101, 6500 HB Nijmegen, The Netherlands. E-mail: J.Jansen@dent.umcn.nl*
†*These authors contributed equally to this study.*

Research efforts in the past decade have focused on enhancing the degradation of apatite CPC by introducing porosity within the ceramic matrix. Initial efforts utilized foaming agents (e.g. CO_2) that induce the formation of gas bubbles within the CPC during setting (del Real *et al.*, 2002). For reasons of lack of control on pore size and pore distribution, the inclusion of rapidly degrading microspheres was explored. From multiple polymeric materials, poly(lactic-co-glycolic acid) (PLGA) was demonstrated to have most suitable properties regarding both control on degradation (Habraken *et al.*, 2006) and tissue response (Liao *et al.*, 2011). More specifically, the amount of PLGA microspheres (Lopez-Heredia *et al.*, 2012a), PLGA molecular weight and end-group functionalization were demonstrated to have significant effects on the degradation of PLGA microspheres, leading to fast degradation and substantial bone formation for CPC formulations containing PLGA microspheres with a low molecular weight ($<$ 20 kDa) and acid-terminated polymer chains (Félix Lanao *et al.*, 2011a, 2011b).

To date, the effects of pore dimensions obtained after hydrolytic degradation of PLGA microspheres within CPC have not been addressed. Several discrepancies exist with respect to adequate pore size of ceramic materials to allow bone ingrowth and substantial bone formation. A number of reports have concluded that pore dimensions of at least 50 μm are required to allow cell ingrowth and blood vessel ingrowth to aid in scaffold degradation (Bohner and Baumgart, 2004; Link *et al.*, 2008). In contrast, other studies have concluded that human osteoblasts can penetrate into interconnective porosity if the pores are $>$ 20 μm in size (Lu *et al.*, 1999), or even that pore size does not significantly affect tissue ingowth and the resorption of calcium phosphate scaffolds (von Doernberg *et al.*, 2006).

In view of these controversial results, the aim of the current study was to elucidate the true effect of pore dimensions within CPC on bone formation after injection of CPC/PLGA in a guinea pig tibial intramedullary model. To this end, injectable CPC/PLGA formulations were prepared using PLGA microspheres with either a small (~25 μm) or a large (~100 μm) diameter, which were incorporated at a 20:80 ratio (wt%) within apatite CPC. Both CPC/PLGA formulations were injected into a marrow-ablated tibial intramedullary cavity and, after an implantation period of 12 weeks, histology and histomorphometry were used to address bone formation.

2. Materials and methods

2.1. Materials

The chemical composition of the cement consisted of commercially available calcium phosphate powders: 85% w/w α-tricalcium phosphate (α-TCP; CAM Implants BV, Leiden, The Netherlands), 10% w/w dicalcium phosphate anhydrous (DCPA; J. T. Baker Chemical Co., Phillipsburg, USA) and 5% w/w precipitated hydroxyapatite (pHA; Merck, Darmstadt, Germany). An aqueous solution of 2% Na_2HPO_4 (Merck) was used as the liquid component. Poly (lactic-*co*-glycolic acid) (PLGA; Purasorb® PDLG 5002A (MW 17 kDa, acid-terminated, L:G = 50:50) was provided by Purac Biomaterials (Gorinchem, The Netherlands). For the preparation of the PLGA microspheres, polyvinyl alcohol (PVA; 88% hydrolysed, MW 22.000, Acros, Geel, Belgium), isopropanol (IPN; analytic grade, Merck) and dichloromethane (DCM; analytic grade, Merck) were used.

2.2. Preparation of PLGA microspheres

PLGA microspheres were prepared using a water/oil/water (w/o/w) double emulsion solvent evaporation technique. A total of 1.0 g PLGA was dissolved in 4 ml DCM in a 20 ml glass tube, 0.5 ml milliQ water was added and the emulsion was emulsified (small diameter microspheres, 8000 rpm for 90 s; large diameter microspheres, 3200 rpm for 90 s) with an emulsifier (IKA® T25 digital ultra-Turrax®, IKA® Werke GMBH and Co. KG, Germany). Subsequently, 6 ml 0.3% PVA solution was added and emulsified again at 8000 rpm for another 90 s. The content of the 50 ml tube was transferred to a stirred 1000 ml beaker containing 394 ml 0.3% PVA. Following addition of 400 ml 2% IPN solution, the suspension was stirred for 1 h. After the microspheres had been allowed to settle for 15 min, the suspension was centrifuged and the supernatant solution was decanted. This washing procedure was repeated twice and the microspheres were collected, lyophilized for 24 h and stored at −20°C.

2.3. Characterization of PLGA microspheres

The morphology and size distribution of the PLGA microspheres was determined by light microscopy. Microspheres were suspended in water and images were acquired using an optical microscope equipped with a digital camera (Leica/Leitz DM RBE Microscope system, Leica Microsystems AG, Wetzlar, Germany). Thereafter, digital image software (Leica Qwin®, Leica Microsystems) was used to determine microsphere size distribution, using a sample size of $>$ 300 microspheres. In addition, microsphere morphology was assessed using scanning electron microscopy (SEM; JEOL 6310) at an accelerating voltage of 10 kV, which was performed at the Microscope Imaging Centre (MIC) of the Nijmegen Centre for Molecular Life Sciences (NCMLS).

2.4. Preparation of CPC/PLGA formulations

CPC/PLGA formulations were generated by adding 0.2 g PLGA microspheres to 0.8 g CPC powder inside a 2 ml plastic syringe. The two different CPC/PLGA formulations so created contained either small microspheres (CPC/PLGA-S) or large microspheres (CPC/PLGA-L). All syringes were

sealed with a closed tip and sterilized using γ-irradiation (25–50 kGy; Isotron BV, Ede, The Netherlands).

2.5. Characterization of CPC/PLGA composites

Physicochemical characterization of the CPC/PLGA formulations was conducted as described previously (Habraken *et al*., 2006; Félix Lanao *et al*., 2011a). Briefly, the porosity of these formulations was assessed by preparing preset, cylindrical scaffolds ($n = 3$) using Teflon moulds, after which the diameter, height and weight of these scaffolds were measured before and after heating the scaffolds at 650°C for 2 h. The total porosity and macroporosity were derived using equations described previously (Zuo *et al*., 2010).

Since the effect of PLGA particles on setting (Habraken *et al*., 2006), strength (Habraken *et al*., 2006, Lopez-Heredia *et al*., 2012a) and degradation (Félix Lanao *et al*., 2011a) of CPC has been previously reported, these types of characterization study have not been included in this paper.

2.6. Animal model and implantation procedure

Twenty female guinea pigs (Harlan, Horst, The Netherlands), aged 7 months, were used as experimental animals, each receiving unilateral surgery of only the right tibia. The study was approved by the Animal Ethics Committee of Nijmegen, The Netherlands (Approval No. DEC 2009–127) and national guidelines for the care and use of laboratory animals were respected. General anaesthesia was maintained by 0.5–2% isoflurane administered through inhalation, and the depth of anaesthesia was monitored by a lack of response to toe pinch and by monitoring the depth of respiration. To reduce perioperative infection risk and minimize postoperative discomfort, antibiotic prophylaxis (Baytril®, 2.5%; Enrofloxacin, 10 mg/kg) was administered prior to surgery and daily on days 1–3 postsurgery.

For injection of the CPC/PLGA formulations, the animal was immobilized on its back and the right hindlimb was shaved, washed and disinfected with povidone–iodine. Two small longitudinal incisions were made along the distal and proximal tibial diaphysis. After exposure of the tibia, a full-thickness cortical defect (2.0 mm in diameter) was made in both distal and proximal sites, using low rational drill speeds (max. 450 rpm) and constant saline irrigation. The content of the marrow space was evacuated by curettage using a dental file and repeated irrigation with saline; a sterile cotton gauze was applied to stop bleeding. Then, the CPC/PLGA formulation was prepared within the operating theatre by adding 0.38 ml sterile 2% Na_2HPO_4 solution to a syringe containing either CPC/PLGA-S or CPC/PLGA-L and mixed vigorously for 30 s (Silamat® mixing apparatus, Vivadent, Schaan, Liechtenstein). After removing the tip of the syringe, the CPC/PLGA formulation was immediately injected into the bone marrow-ablated tibia medullar cavity. The distal hole served as the entrance and the proximal hole as the evacuation site for CPC/PLGA (Figure 1a). After injection, the CPC/PLGA formulation was allowed to set for 10 min, after which the excess material was removed with a spatula. Subsequently, the soft tissues were closed in two layers, using resorbable sutures (monocryl 4–0). After surgery, the animals were housed in groups and given water and chow *ad libitum*. The animals were physically examined on a daily basis during the first 10 days postsurgery, with focus on body weight, infection and adverse reactions. At 12 weeks postimplantation, the animals were euthanized by an injection of concentrated sodium pentobarbital.

2.7. Histological and histomorphometrical evaluation

Immediately after euthanasia, the tibias were retrieved and fixed in 4% formaldehyde for 1 week and dehydrated

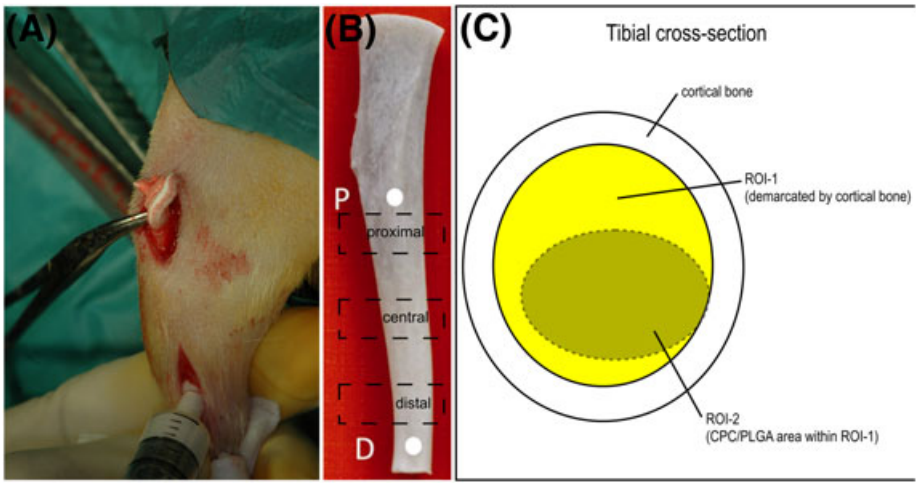

Figure 1. (A) Injection of CPC/PLGA into the bone marrow-ablated tibia medullar cavity, where the distal hole served as entrance and the proximal one as evacuation site. (B) Three different regions of the tibia defined for histological analysis; P, proximally and D, distally drilled holes. (C) Regions of interest (ROI); ROI-1 demarcates the intramedullary cavity and ROI-2 refers to the CPC–PLGA area within ROI-1

DOI: 10.1002/term

in a graded series of alcohols. After dehydration, the tibias were cut into two parts, proximal and distal. These parts were alternately allocated to two groups: the first group was composed of proximal halves of even tibias and distal halves of odd tibias, the second group was composed of distal halves of even and proximal halves of odd tibias. The first group was left non-decalcified and embedded in polymethyl methacrylate (PMMA). After polymerization, these blocks were used to prepare thin (10 μm) sections ($n = 3$ for each half tibia), using a Leica SP1600 saw microtome. These sections were made perpendicular to the long axis of the tibia and stained with methylene blue/basic fuchsin. The second group of specimens was decalcified with a specific-purpose apparatus (TDE30, Sakura) and dehydrated in a graded series of ethanols. Finally, the specimens were embedded in paraffin and histological sections were prepared using a standard microtome (RM 2165, Leica) in three different regions of the tibia (Figure 1b), close to the distal entry site, in the central part of the diaphysis and close to the proximal exit site. For each region, a total of six sections were stained with haematoxylin and eosin (H&E) and another six sections were stained with Elastica van Gieson (EVG).

Histological evaluation was done using an optical microscope (Axio Imager Microscope Z1, Carl Zeiss Microimaging GmbH, Göttingen, Germany) and consisted of a concise description of the observed specimens.

Histomorphometrical evaluation was performed using EVG-stained paraffin sections in order to have the highest resolution for detecting bone formation inside the medullar cavity. For quantification, three sections of each region per tibia (Figure 1b) were used. Two regions of interest (ROIs) were set: ROI-1 was set to demarcate the intramedullary cavity; ROI-2 was determined based on morphological and colour discrimination between tissue and ceramic matrix within ROI-1 (Figure 1c). The bone area within both these ROIs was measured using Leica Qwin software (Leica Microsystems Imaging Solution, Cambridge, UK).

2.8. Statistical analysis

Statistical analyses were performed using GraphPad Instat 3.05 software (GraphPad Software Inc., San Diego, CA, USA). The statistical comparison between the two CPC/PLGA formulations was performed using an unpaired Student's *t*-test. Alternatively, a one-way ANOVA was used to analyse bone formation at different regions. Differences were considered significant at $p < 0.05$.

3. Results

3.1. Characterization of PLGA microspheres and CPC/PLGA composites

SEM images of the prepared PLGA microspheres and obtained CPC/PLGA composites are depicted in Figure 1. Both small and large PLGA microspheres showed a spherical morphology. The size distribution measurements revealed an average microsphere diameter of 27 ± 7 μm for small and 100 ± 35 μm for large PLGA microspheres ($p < 0.05$).

When incorporated within CPC, the morphology of preset CPC/PLGA scaffolds showed a tight packing of the PLGA microspheres. Furthermore, the PLGA microspheres were distributed homogeneously throughout the CPC

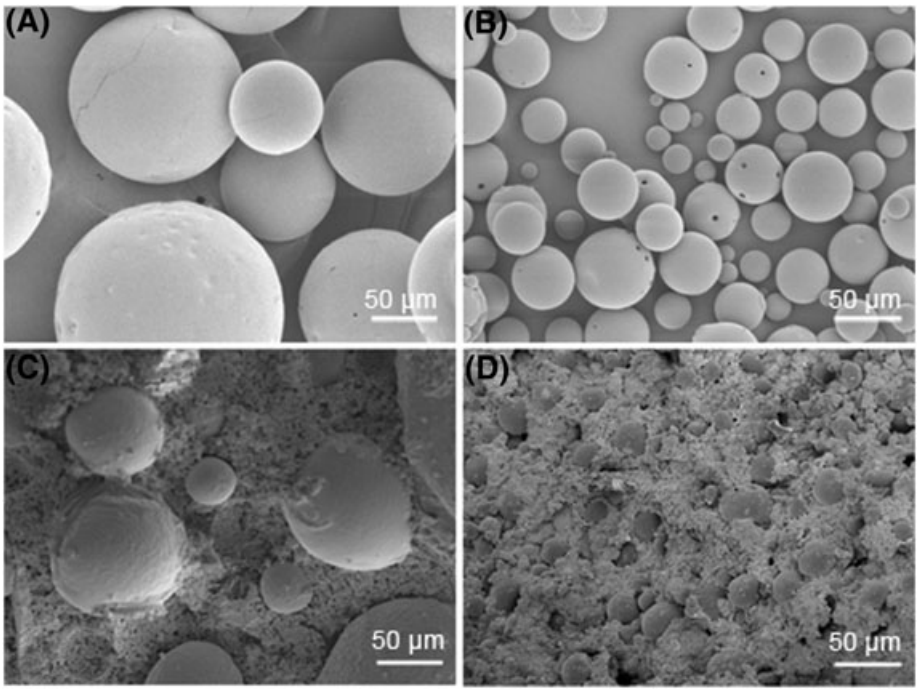

Figure 2. SEM images: (A) large PLGA microspheres; (B) small PLGA microspheres; (C) CPC/PLGA-L and (D) CPC/PLGA-S

DOI: 10.1002/term

matrix. An apparent increase in interconnection of PLGA microspheres was observed for CPC/PLGA-S compared to CPC/PLGA-L (Figure 2b, d). The total porosities of CPC/PLGA-S and CPC/PLGA-L were similar, with values of. 67.2 ± 1.5% and 66.9 ± 0.6%, respectively ($p > 0.05$), to which the PLGA microspheres contribute in the form of macroporosity of ~45% (Table 1).

3.2. Clinical observations

The surgical procedure was uneventful for all animals. In the course of the implantation period, three animals (two CPC/PLGA-L and one CPC/PLGA-S) were sacrificed due to a tibial fracture. The other 17 animals remained in good health and did not show any wound complications (i.e. signs of inflammation, such as swelling and redness). After the 12-week implantation period, a total of 17 tibias with injected CPC/PLGA formulations (i.e. nine CPC/PLGA-S and eight CPC/PLGA-L) were retrieved. An overview of the number of implants placed and retrieved is given in Table 2.

3.3. Histology and histomorphometry

3.3.1. Descriptive histology

PMMA sections (Figure 3) demonstrated the presence of CPC/PLGA within the intramedullary cavity (dark areas) at the distal side, with full contact with the cortical bone. In contrast, the proximal side showed less contact between CPC/PLGA and the cortical bone, leaving voids. These voids were partially filled with newly-formed bone (Figure 3C). Since the PMMA sections did not allow accurate discrimination between CPC and tissue, paraffin-embedded sections of decalcified specimens were used. EVG-stained sections clearly showed abundant bone formation within the intramedullary cavity (Figure 4). More specifically, H&E-stained sections (Figure 5) allowed identification of the CPC matrix and showed two distinct morphologies, with trabecular-like bone structures in the areas outside the CPC matrix (either not present or degraded) and round bone structures inside the CPC matrix (Figure 5). For CPC/PLGA-L, these round bone structures

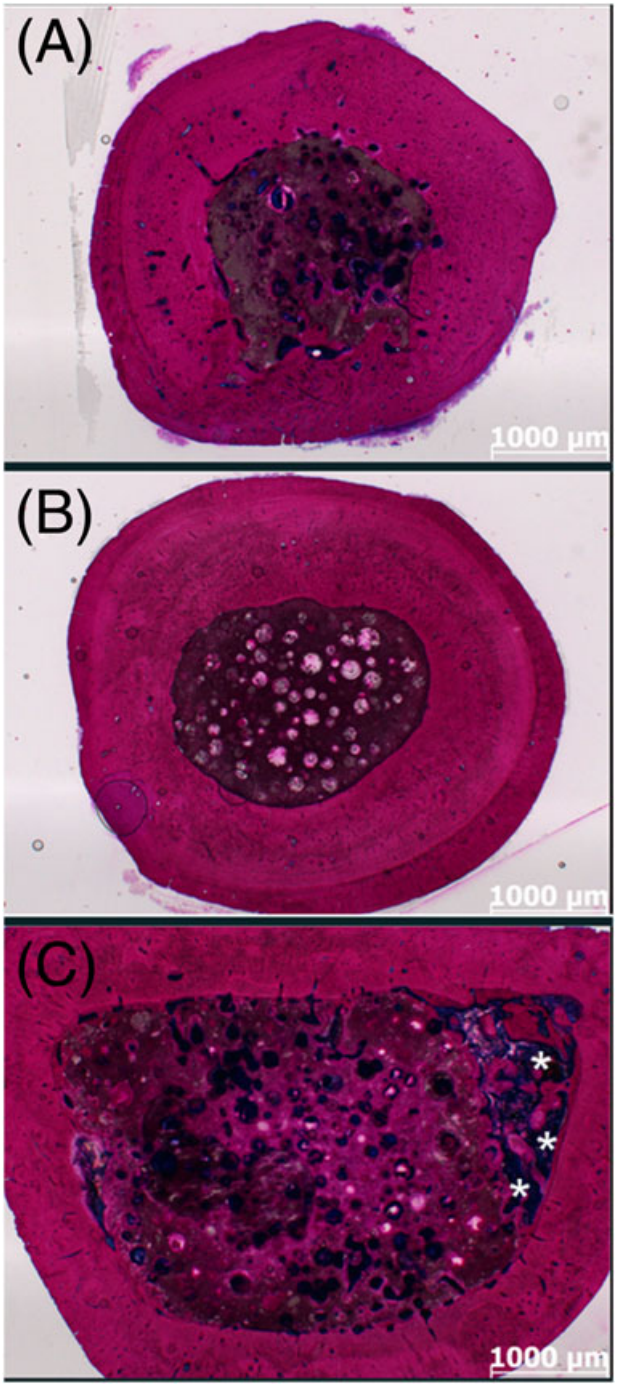

Figure 3. Representative histological images of PMMA sections: (A) proximal, (B) central and (C) distal regions of the tibia containing CPC/PLGA-L composites. *Voids between the CPC/PLGA and cortical bone in the distal region

Table 1. Characteristics of PLGA microspheres and CPC/PLGA formulations

Name	CPC/PLGA -S	CPC/PLGA-L
Average size microspheres (µm)	27 ±7	100 ± 35
Microspheres (wt%)	20	20
Porosity (%)	67.2 ± 1.5	66.9 ± 0.6
Macroporosity (%)	44.5 ± 2.5	44.1 ± 1.0

Table 2. Experimental groups, number of implants placed and retrieved

Experimental group	Composition	Implants placed	Implants retrieved
CPC/PLGA-L	CPC with 20 wt% large PLGA microspheres	10	8*
CPC/PLGA-S	CPC with 20 wt% small PLGA microspheres	10	9*

*Deviation from number of implants placed due to fracture of the tibia during implantation period.

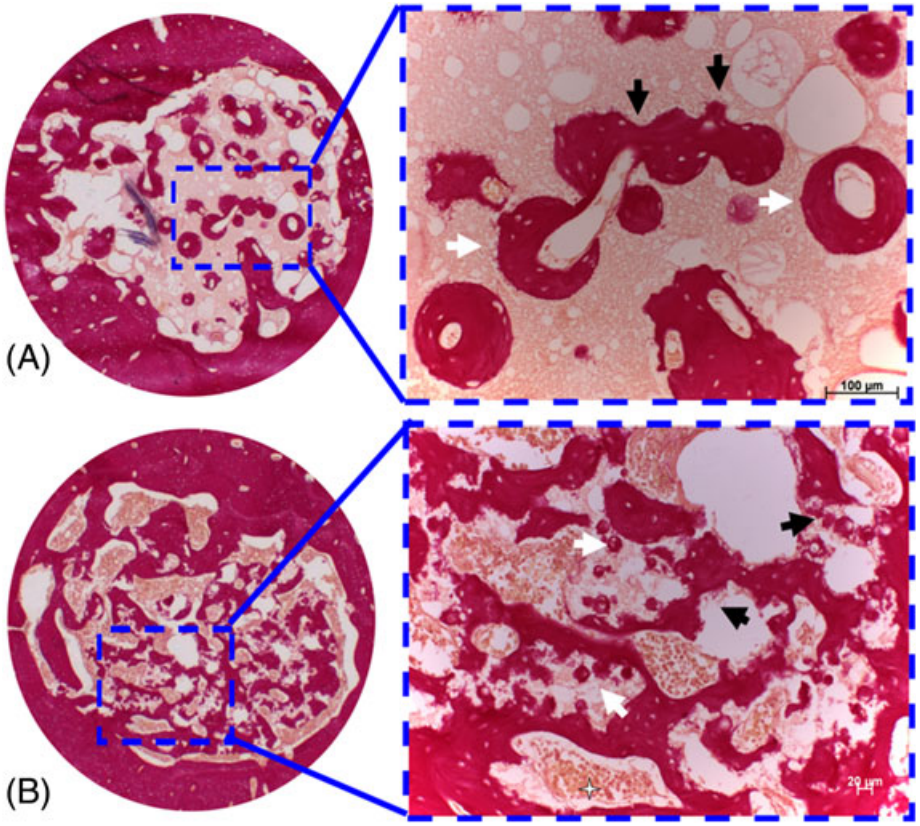

Figure 4. Representative EVG-stained sections: (A) CPC/PLGA-L and (B) CPC/PLGA-S: black arrows, interconnected pores filled with bone; white arrows, pores filled with bone that maintain the original size and morphology of PLGA microspheres

showed embedded osteocytes within the bone matrix and had dimensions ~100 µm in diameter, in which cavities with marrow-like tissue were frequently observed. For CPC/PLGA-S, much smaller dimensions for these round bone structures were observed (~20 µm), which had frequently fused into trabecular-like bone structures. Marrow-like tissue was observed between these larger trabecular-like bone structures inside the CPC matrix. The newly-formed bone always showed (also in the round bone structures) the presence of osteocytes.

3.3.2. Histomophometrical evaluation

Bone formation was evaluated within two different ROIs, which covered either the entire intramedullary cavity or the area of the CPC matrix (Figure 1c). The results on bone formation are depicted in Figure 6.

Total bone formation within ROI-1 (i.e. average of measurements at different regions, distal, central and proximal; Figure 6A) for CPC/PLGA-S and CPC/PLGA-L was 26.9 ± 19.2% and 24.4 ± 18.7%, respectively ($p > 0.05$). Total bone formation measurements within ROI-2 (i.e. average of measurements at different regions, distal, central and proximal; Figure 6A) revealed that CPC/PLGA-S showed significantly higher amounts of bone (23.8 ± 15.6%) compared to CPC/PLGA-L (9.9 ± 7.9%; $p = 0.0093$). (Figure 6A).

For different regions of the tibial intramedullary cavity (i.e. distal, central or proximal), both CPC/PLGA formulations demonstrated similar amounts of bone within ROI-1 ($p > 0.05$; Figure 6B), whereas region- and CPC/PLGA formulation-related differences were observed within ROI-2 (Figure 6C). Region-related specification for both CPC/PLGA-formulations showed significantly less bone formation in the central region compared to both the distal and proximal regions ($p < 0.05$). Alternatively, the formulation-related specification showed significantly more bone formation for CPC/PLGA-S compared to CPC/PLGA-L in both the proximal and distal regions ($p < 0.05$) but not in the central region ($p > 0.05$).

4. Discussion

The aim of the present study was to evaluate the effect of PLGA microsphere dimensions on bone formation after injection of CPC/PLGA in a guinea pig tibial intramedullary model. The reported results evidently reveal that bone tissue can grow into porosities within CPC, as created by the degradation of PLGA microspheres, with dimensions as small as ~25 µm. Importantly, total bone formation within the CPC/PLGA bone substitute demonstrated two-fold bone formation for CPC containing small PLGA microspheres compared to CPC containing large PLGA microspheres. Additionally, the pattern of bone and marrow formation showed distinct differences depending on the dimensions of the PLGA microspheres within the CPC–PLGA formulations.

Compared to other small animal models used for the preclinical evaluation of bone substitute performance

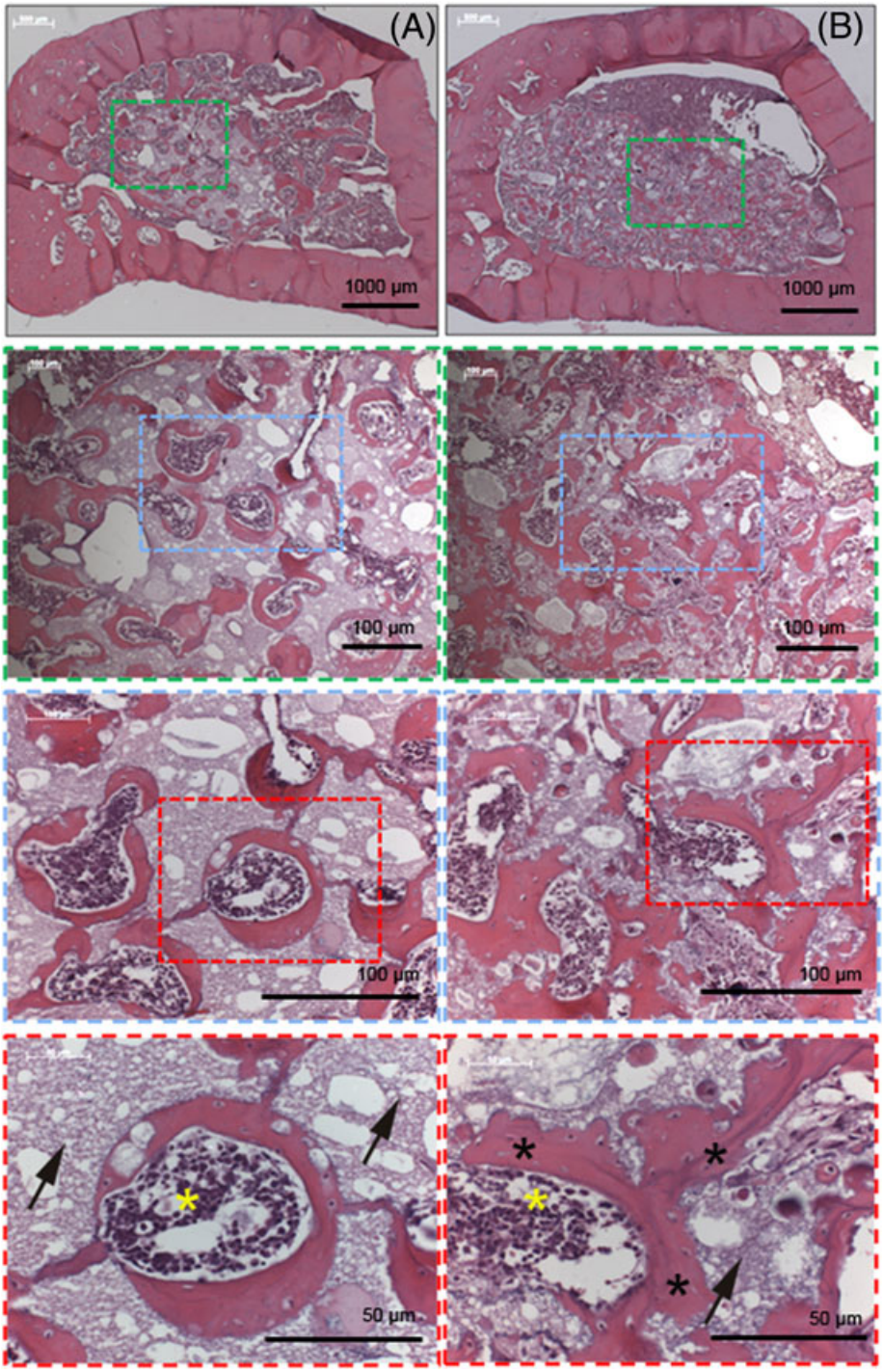

Figure 5. Representative H&E-stained histological sections of the proximal region with (A) CPC/PLGA-L and (B) CPC/PLGA-S. Lower panels are magnifications of the boxes indicated in the image above. Yellow and black asterisks indicate the presence of marrow-like tissue and trabecular-like bone structures containing osteocytes, respectively; black arrows, remnants of CPC

(e.g. murine calvaria and femoral epiphysis) (van de Watering *et al*., 2012; Plachokova *et al*., 2008), the presently used model comprises several differences. First, an intramedullary cavity is not a bony site in the sense that the native tissue in that area consists of bone. As such, it cannot be considered as a bone defect, but rather as a bone augmentation model, in which native bone tissue is activated from the endosteal site following bone marrow ablation (Amsel *et al*., 1969; Bab, 1995). Second, the tissue surrounding the site of injection is different from that in normal bone defect and bone augmentation models. Whereas in these latter models the site is surrounded by either bone tissue or soft tissue, the intramedullary cavity is composed of bone marrow and fat tissue, while being circumferentially surrounded by cortical bone. Despite this difference with regular bone defect and bone augmentation models, the guinea pig tibial intramedullary model was chosen because it allows that the cement can indeed be tested as an injectable material and also provides large-sized histological specimens, which

DOI: 10.1002/term

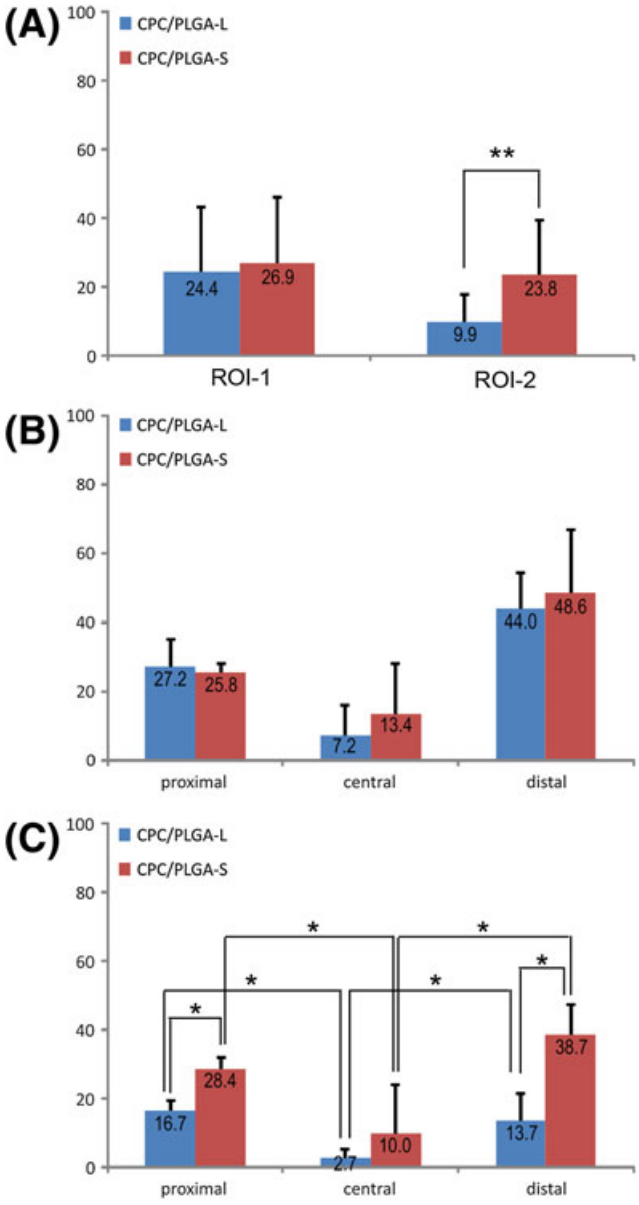

Figure 6. Quantification of bone formation. (A) total bone formation in ROI-1 (i.e. average of all different levels at which sections were made, distal, central and proximal) and total bone formation in ROI-2 (i.e. average of all the different levels at which sections were made, distal, central and proximal). (B) Bone formation in ROI-1 at the different levels. (C) Bone formation in ROI-2 at the different levels

can be subjected to multiple approaches for analysis (i.e. embedding in both PMMA and paraffin of alternate tibial halves).

Regarding the quantification of CPC/PLGA degradation, the intramedullary model has several limitations. For a reliable assessment, it is mandatory to achieve complete filling and setting of the injectable CPC/PLGA bone substitute. Within a secluded cavity connected to liquid areas (i.e. bone marrow) proximally and distally, it remains speculative if that can be achieved. It needs to be emphasized that, for regular bone defect models, the defect is maximally dried to avoid interference of bodily fluids with filling and setting (Félix Lanao *et al.*, 2012; Oortgiesen *et al.*, 2013).

Examination of the PMMA sections revealed that both CPC/PLGA formulations were still present within the intramedullary cavity at the end of the 12 weeks implantation time. Due to the high density of the CPC/PLGA composite material, the relative thickness of PMMA sections and artifacts caused by staining, analysis of bone formation using PMMA embedding is inaccurate (Lopez-Heredia *et al.*, 2012b). In contrast, H&E and EVG staining of decalcified paraffin sections indicated the presence of abundant bone formation within the CPC matrix. As such, these results demonstrate the importance of combined analysis (calcified/decalcified) for a complete understanding of the two processes of material degradation and bone formation.

The quantitative assessment of bone formation showed no differences in total bone formation within the tibial intramedullary cavity related to PLGA microsphere dimensions. However, within the CPC matrix, bone formation of CPC/PLGA with small PLGA microspheres was > two-fold higher compared to CPC/PLGA with large PLGA microspheres. Further specification of this difference showed that especially the proximal and distal regions of the tibial intramedullary cavity contributed to this result. This effect is likely to be caused by bone marrow left at the proximal and distal ends of the intramedullary cavity after the ablation procedure. This remaining bone marrow could have acted as an initiator for new bone formation.

Review of previously performed studies indicate that no conclusive statement can be made about the scaffold requirements (porosity, composition, etc.) to allow bone ingrowth. For example, *in vivo* studies with ectopic implantation of preset CPC/PLGA scaffolds have shown that soft tissue ingrowth throughout the scaffold is feasible with PLGA microsphere sizes > 50 μm incorporated at 20 wt% (Link *et al.*, 2008). Alternatively, the assessment of bone ingrowth into biomaterials with different compositions (i.e. sintered hydroxyapatite with 'cellular' or 'strut-like' designs) and porosity characteristics (i.e. porosity 32–56%, pore radius 71–167 μm) showed that pore size was strongly correlated to bone ingrowth, with a strong enhancement of bone ingrowth when pore diameters exceeded 100 μm (Jones *et al.*, 2007). Also, one of our recent studies indicated that a CPC/PLGA formulation with 30 wt% PLGA microspheres of 40 μm would be optimal regarding mechanical properties, porosity and interconnectivity (Lopez-Heredia *et al.*, 2012a). This inconsistency in observations is confirmed by the present study, which shows that bone ingrowth throughout the material was obtained for an injectable CPC/PLGA formulation with 20 wt% PLGA microspheres of ~25 μm. This formulation even showed significantly more bone formation compared to the CPC/PLGA formulation with 20 wt% PLGA microspheres of ~100 μm, while formulations had a similar total porosity (~67%) to which the PLGA equally contributed (i.e. macroporosity of ~44%). In contrast with previous studies, which reported that small pore sizes (40–80 μm) led to less bone formation than larger pore sizes (200–400 μm) (Bobyn *et al.*, 1980; Galois and Mainard 2004), it seems straightforward to conclude

that a higher pore interconnectivity of the CPC/PLGA-S material caused the currently observed favourable effect on bone ingrowth. However, it has to be emphasized that, in addition to the created macroporosity due to PLGA degradation, CPC/PLGA possesses an intrinsic nanoporosity. Therefore, the majority of CPC/PLGA pores are additionally interconnected via this nanoporosity, which allows for enhanced fluid flow and nutrient circulation within the material. At the same time, the fluid flow circulation can accelerate the transformation as well as degradation of the CPC, resulting in more space for tissue ingrowth.

Within the tibial intramedullary cavity. the response to several ceramic bone substitutes has previously been described to follow a pattern from endosteal bone healing via marrow cavity remodelling to marrow restoration (Schwartz *et al*., 2008). The results of the present study not only show an effect of remaining bone marrow on bone formation, but also demonstrate that marrow regeneration occurred within the CPC matrix. Interestingly, the location of regenerated bone marrow was dependent on the size of the PLGA microparticles: whereas large PLGA microspheres evoked bone formation in round patterns and marrow in the centre, small PLGA microparticles appeared to give rise to trabecular-like bone formation with bone marrow present between such trabeculae. As described in the literature, anatomical restrictions necessitate specific dimensions (i.e. porosity) to allow bone marrow and blood vessel formation (Mastrogiacomo *et al*., 2006; Sicchieri *et al*., 2012). However, this study provides sufficient evidence that new bone formation occurs throughout a CPC matrix with pores of 25 μm in diameter. Therefore, it can be hypothesized that CPC nanoporosity, in combination with the porosity generated after PLGA degradation, provides sufficient space for nutrient diffusion to allow bone cells to survive, with the presence of bone marrow but without the formation of new blood vessels, until further degradation of the CPC matrix. This observation closely resembles the situation that occurs in nature within the cortical bone structures, where the Haversian system contains blood vessels only in the Volkmann's canal. Nutrients diffuse out from the vessel within these canals to the osteocytes in the Haversian system via nano-sized canaliculi.

5. Conclusion

The results of the present study demonstrate that the dimensions of PLGA microspheres within injectable CPC/PLGA have a substantial effect on bone formation. Whereas both small (~25 μm) and large (~100 μm) microspheres allowed bone ingrowth throughout the CPC matrix, a > two-fold higher amount of newly formed bone was observed for CPC/PLGA with small PLGA microspheres within the CPC matrix. Additionally, the pattern of bone and marrow formation showed distinct differences related to PLGA microsphere size. In general, this study demonstrates that PLGA microsphere dimensions of ~25 μm, leading to pores of ~25 μm within CPC, are sufficient for bone ingrowth and allow substantial bone formation. Further, the results demonstrate that PLGA microsphere dimensions provide a tool to control bone formation for injectable CPC/PLGA bone substitutes.

Conflict of interest

The authors have declared that there is no conflict of interest.

Acknowledgements

The authors would like to thank Natasja van Dijk for histological assistance. Scanning electron microscopy was performed at the Microscope Imaging Centre (MIC) of the Nijmegen Centre for Molecular Life Sciences (NCMLS). The authors gratefully acknowledge the support of the SmartMix Programme of The Netherlands Ministry of Economic Affairs and The Netherlands Ministry of Education, Culture and Science.

References

Amsel S, Maniatis A, Tavassoli M, *et al*. 1969; The significance of intramedullary cancellous bone formation in the repair of bone marrow tissue. *Anat Rec* **164**(1): 101–111.

Bab IA. 1995; Postablation bone marrow regeneration: an *in vivo* model to study differential regulation of bone formation and resorption. *Bone* **17**(4): 437–441.

Bobyn JD, Pilliar RM, Cameron HU, *et al*. 1980; The optimum pore size for the fixation of porous-surfaced metal implants by the ingrowth of bone. *Clin Orthop Rel Res* **150**: 263–270.

Bongio M, van den Beucken JJJP, Leeuwenburgh SCG, *et al*. 2010; Development of bone substitute materials: from 'biocompatible' to 'instructive'. *J Mater Chem* **20**(40): 8747–8759.

Bohner M 2010; Design of ceramic-based cements and putties for bone graft substitution. *Eur Cells Mater* **20**: 1–12.

Bohner M, Baumgart F. 2004; Theoretical model to determine the effects of geometrical factors on the resorption of calcium phosphate bone substitutes. *Biomaterials* **25**(17): 3569–3582.

Brown WE, Chow LC. 1986; A new calcium phosphate water-setting cement. In *Cements Research Progress*, Brown PW (ed.). American Ceramic Society: Westerville, OH: USA.

del Real RP, Wolke JG, Vallet-Regi M, *et al*. 2002; A new method to produce macropores in calcium phosphate cements. *Biomaterials* **23**(17): 3673–3680.

Dorozhkin SV. 2010; Bioceramics of calcium orthophosphates. *Biomaterials* **31** (7): 1465–1485.

Félix Lanao RP, Leeuwenburgh SCG, Wolke JGC, *et al*. 2011a; *In vitro* degradation rate of apatitic calcium phosphate cement with incorporated PLGA microspheres. *Acta Biomater* **7**(9): 3459–3468.

Félix Lanao RP, Leeuwenburgh SCG, Wolke JGC, *et al*. 2011b; *In vivo* bone response to fast-degrading, injectable calcium phosphate cements with enhanced *in situ* forming porosity. *Biomaterials* **32**(34): 8839–8847.

Félix Lanao RP, Hoekstra JW, Wolke JG, *et al*. 2012; Porous calcium phosphate cement for alveolar bone regeneration. *J Tissue Eng Regen Med*. doi: 10.1002/term.1546. [Epub ahead of print]

Galois L, Mainard D. 2004; Bone ingrowth into two porous ceramics with different pore sizes: an experimental study. *Acta Orthop Belg* **70**(6): 598–603.

Habraken WJ, Wolke JG, Mikos AG, *et al*. 2006; Injectable PLGA microsphere/calcium phosphate cements: physical properties and degradation characteristics. *J Biomater Sci Polym Ed* **17**(9): 1057–1074.

Jones AC, Arns CH, Sheppard AP, *et al*. 2007; Assessment of bone ingrowth into porous biomaterials using micro-CT. *Biomaterials* **28**(15): 2491–2504.

Kolk A, Handschel J, Drescher W, *et al*. 2012; Current trends and future perspectives of bone substitute materials – from space holders to innovative biomaterials. *J Craniomaxillofac Surg* **40**(8): 706–718.

Kretlow JD, Young S, Klouda L, *et al*. 2009; Injectable biomaterials for regenerating complex craniofacial tissues. *Adv Mater* **21**(32–33): 3368–3393.

Liao H, Walboomers XF, Habraken WJ, *et al*. 2011; Injectable calcium phosphate cement with PLGA, gelatin and PTMC microspheres in a rabbit femoral defect. *Acta Biomater* **7**(4): 1752–1759.

Link DP, van den Dolder J, van den Beucken JJJP, *et al*. 2008; Evaluation of the biocompatibility of calcium phosphate cement/PLGA microparticle composites. *J Biomed Mater Res A* **87**(3): 760–769.

Lopez-Heredia MA, Sariibrahimoglu K, Yang W, *et al*. 2012a; Influence of the pore generator on the evolution of the mechanical properties and the porosity and interconnectivity of a calcium phosphate cement. *Acta Biomater* **8**(1): 404–414.

Lopez-Heredia MA, Bongio M, Cuijpers VM, *et al*. 2012b; Bone formation analysis: effect of quantification procedures on the study outcome. *Tissue Eng C Methods* **18**(5): 369–373.

Lu JX, Flautre B, Anselme K, *et al*. 1999; Role of interconnections in porous bioceramics on bone recolonization *in vitro* and *in vivo*. *J Mater Sci Mater Med* **10**(2): 111–120.

Mastrogiacomo M, Scaglione S, Martinetti R, *et al*. 2006; Role of scaffold internal structure on *in vivo* bone formation in macroporous calcium phosphate bioceramics. *Biomaterials* **27**(17): 3230–3237.

Oortgiesen DA, Meijer GJ, Bronckers AL, *et al*. 2013; Regeneration of the periodontium using enamel matrix derivative in combination with an injectable bone cement. *Clin Oral Invest* **17**(2): 411–421.

Plachokova AS, van den Dolder J, Jansen JA. 2008; The bone-regenerative properties of Emdogain adsorbed onto poly(D,L-lactic-coglycolic acid)/calcium phosphate composites in an ectopic and an orthotopic rat model. *J Periodont Res* **43**(1): 55–63.

Schwartz Z, Doukarsky-Marx T, Nasatzky E, *et al*. 2008; Differential effects of bone graft substitutes on regeneration of bone marrow. *Clin Oral Implant Res* **19**(12): 1233–1245.

Sicchieri LG, Crippa GE, de Oliveira PT, *et al*. 2012; Pore size regulates cell and tissue interactions with PLGA–CaP scaffolds used for bone engineering. *J Tissue Eng Regen Med* **6**(2): 155–162.

Tamimi F, Sheikh Z, Barralet J. 2012; Dicalcium phosphate cements: brushite and monetite. *Acta Biomater* **8**(2): 474–487.

van de Watering FC, van den Beucken JJ, Walboomers XF, *et al*. 2012; Calcium phosphate/poly(D,L-lactic-co-glycolic acid) composite bone substitute materials: evaluation of temporal degradation and bone ingrowth in a rat critical-sized cranial defect. *Clin Oral Implant Res* **23**(2): 151–159.

von Doernberg MC, von Rechenberg B, Bohner M, *et al*. 2006; *In vivo* behavior of calcium phosphate scaffolds with four different pore sizes. *Biomaterials* **27**(30): 5186–5198.

Zuo Y, Yang F, Wolke JG, Li Y, *et al*. 2010; Incorporation of biodegradable electrospun fibers into calcium phosphate cement for bone regeneration. *Acta Biomater* **6**(4): 1238–1247.